MODELING MULTIPHASE FLUID FLOW IN UNCONVENTIONAL RESERVOIRS

Gabriela B. Savioli[a]**, Juan E. Santos**[a,b]**, Patricia Gauzellino**[c] **and Miguel Lavia**[a]

[a]*Universidad de Buenos Aires, Facultad de Ingeniería, Instituto del Gas y del Petróleo, Av. Las Heras 2214 Piso 3 C1127AAR Buenos Aires, Argentina, gsavioli@fi.uba.ar*

[b]*Department of Mathematics, Purdue University, 150 N. University Street, West Lafayette, Indiana, 47907-2067, USA, jsantos48@gmail.com*

[c]*Facultad de Ciencias Astronómicas y Geofísicas,Universidad Nacional de La Plata*

Keywords: black oil, unconventional reservoir, fracking

Abstract. A hydrocarbon reservoir is defined as *unconventional* when it requires special completion techniques outside the conventional ones. In particular, tight gas, shale gas and shale oil reservoirs are unconventional due to their very low or ultra low permeability. To allow oil and gas production, the formation has to be fractured injecting fluids at high pressures. Fluid injection increases the pore pressure and, consequently, the effective stress in rocks. In this way, a set of fractures are generated creating pathways where hydrocarbons can flow to a producing well. To simulate fracture propagation, a breakdown pressure criterion is applied: during injection, once pore pressure becomes greater than a breakdown value on a certain cell, that cell is fractured increasing permeability and porosity values. The objective of this work is to test a simple numerical model of hydraulic fracture generation in unconventional reservoirs that combines a multiphase flow simulator with the breakdown pressure criterion. The multiphase flow through porous media is described by the well-known Black-Oil formulation, which uses as a simplified thermodynamic model, the PVT data: formation volume factors and gas solubility in oil and water. The numerical solution is obtained applying an IMPES (IMplicit Pressure Explicit Saturation) finite difference technique. The multiphase flow simulator is used to model the fracture propagation in a tight gas reservoir. In the examples we consider a very low permeability porous media with natural fractures located in the same plane. We analyze the hydraulic fracture advance in that plane and its interaction with natural fractures.

1   INTRODUCTION

Hydraulic fracturing is a process that involves injecting fluids under high pressure into a reservoir via the well. The objective is to create new fractures in the formation as well as increase the size, extent and connectivity of existing natural fractures thus creating a pathway by which the hydrocarbons can flow to the wellbore (Riahi and Damjanac, 2013). Sand or ceramic materia in fine grains are pumped with the fluids in order to maintain the hydraulic fracture open, once fluid injection stops and porous pressure start relaxing. This technique allows to enhance the fluid flow from the formation to the wellbore and consequently the oil or gas production. In unconventional reservoirs (tight or shale), hydraulic fracturing turns out to be indispensable for the well to become productive (Nagel et al., 2013).

Rigorous modeling of hydraulic fracturing can be seen in Wangen (2011), based on Biot's equation and a finite element representation of the fracture pressure; and also in Pak and Chan (2008), where a fully coupled thermal hydro-mechanical model is developed. A numerical complex fracture network model of a shale gas reservoir with large amounts of natural fractures can be seen in Zhao et al. (2014).

In this work we select a simplified approach to simulate fluid injection and fracture generation: we apply the well known Black-Oil formulation (Aziz and Settari, 1985; Fanchi, 1997) to simulate the simultaneous flow of water and gas in our unconventional reservoir. The simulator is run through different stages: as reservoir pressure increases and exceeds a limit value, petrophysical properties are updated and a new run begins. The final fluid pressures and saturations computed by the fluid simulator are used as initial values of the next run. The changes in permeability and porosity due to the fracking procedure and the presence of injected fluids will change the seismic response (Sena et al., 2011).

This work presents the simulations of water injection and fracture generation in a tight gas reservoir. Commonly, in this type of reservoirs the fracking process produce bi-wing and planar fractures perpendicular to the minimum principal stress (Wang and Zhang, 1998). This work is a starting point that will enable us to continue working in estimating the fracture propagation. In a second stage we will use the resulting static model and the black oil simulator to predict hydrocarbon production through the fractured porous media.

2   METHODOLOGY

2.1   Gas - water flow model in porous media

To simulate water injection into a low permeability gas reservoir, we apply the well known Black-Oil formulation to two-phase (gas phase, subindex g, and aqueous phase, subindex w) and two component (Gas and $Water$) fluid flow. In this approach, Gas component may dissolve in the aqueous phase but $Water$ is not allowed to vaporize into the gas phase. The differential equations are obtained by combining the mass conservation equations with Darcy's empirical Law. The mass conservation equations are:

1. For the Gas component,

$$-\nabla \cdot \left(\rho_g \, v_g + C_{g,w} \, \rho_w \, v_w \right) + q_g = \frac{\partial \left[\phi \left(\rho_g S_g + C_{g,w} \, \rho_w \, S_w \right) \right]}{\partial t}; \tag{1}$$

2. for the $Water$ component,

$$-\nabla \cdot (C_{w,w}\, \rho_w\, v_w) + q_w = \frac{\partial \left[\phi(C_{w,w}\, \rho_w\, S_w) \right]}{\partial t}, \tag{2}$$

where ρ is density at reservoir conditions, v is Darcy velocity, S is saturation, q mass rate of injection per unit volume and ϕ is porosity. $C_{g,w}$, $C_{w,w}$ are the mass fractions of Gas and $Water$ in the aqueous phase, respectively. In the Black-Oil formulation these fractions are computed using a simplified thermodynamic model as

$$C_{g,w} = \frac{R_s\, \rho_g^{SC}}{B_w\, \rho_w}, \quad C_{w,w} = \frac{\rho_w^{SC}}{B_w \rho_w}, \quad \rho_g = \frac{\rho_g^{SC}}{B_g} \tag{3}$$

where R_s (Gas solubility in aqueous phase), B_g (Gas formation volume factor) and B_w ($Water$ formation volume factor) are the PVT data. Also ρ_g^{SC} and ρ_w^{SC} are the gas and water densities at standard conditions. PVT data can be obtainesd by laboratory measurements or applying correlations (Bidner, 2001).

The Darcy's Law for two phase flow (Aziz and Settari, 1985; Jones, 1962) gives the momentum balance for the fluids,

$$v_g = -\underline{\kappa}\frac{\kappa_{rg}}{\eta_g}(\nabla p_g - \rho_g g \nabla D), \tag{4}$$

$$v_w = -\underline{\kappa}\frac{\kappa_{rw}}{\eta_w}(\nabla p_w - \rho_w g \nabla D), \tag{5}$$

where D indicates depth, generally identified with the coordinate z, and g is the gravity constant. Also, p_g, p_w are the fluid pressures and $\underline{\kappa}$ is the absolute permeability tensor, assumed to be diagonal $\underline{\kappa} = \mathrm{diag}(\kappa_x, \kappa_y, \kappa_z)$. For $\beta = g, w$, the functions $k_{r\beta}$ and η_β are the relative permeability and viscosity of the β-phase, respectively. The relative permeability $k_{r\beta}$ is function of fluid saturation. Although Darcy's Law has been obtained empirically, it can be deduced from the Navier Stokes' equation for newtonian fluids (Bear, 1972).

Replacing equations (3)-(5) into equations (1)-(2) and dividing by ρ_g^{SC} and ρ_w^{SC}, the following nonlinear system of partial differential equations is obtained,

$$\nabla \cdot (\underline{\kappa}(\frac{\kappa_{rg}}{B_g \eta_g}(\nabla p_g - \rho_g g \nabla D) + \frac{R_s \kappa_{rw}}{B_w \eta_w}(\nabla p_w - \rho_w g \nabla D))) + \frac{q_g}{\rho_g^{SC}}$$
$$= \frac{\partial \left[\phi \left(\dfrac{S_g}{B_g} + \dfrac{R_s S_w}{B_w} \right) \right]}{\partial t}, \tag{6}$$

$$\nabla \cdot (\underline{\kappa}\frac{\kappa_{rw}}{B_w \eta_w}(\nabla p_w - \rho_w g \nabla D)) + \frac{q_w}{\rho_w^{SC}} = \frac{\partial \left[\phi\dfrac{S_w}{B_w} \right]}{\partial t}. \tag{7}$$

Two algebraic equations relating the saturations and pressures, complete the system:

$$S_w + S_g = 1, \qquad p_g - p_w = P_C(S_w), \tag{8}$$

where P_C is the capillary pressure.

The unknowns for the Black-Oil model are the fluid pressures p_g, p_w and the saturations S_g, S_w for the gas and aqueous phases, respectively. This flow model does not take into account chemical reactions.

The numerical solution is obtained with public-domain software BOAST (Fanchi, 1997) which solves the differential equations using the IMPES algorithm (IMplicit Pressure Explicit Saturation), based on a finite difference technique (Aziz and Settari, 1985). The basic idea of IMPES is to replace equation (6) by a combination of the flow equations, therefore equation (6) multiplied by B_g and equation (7) multiplied by $(B_w - R_s B_g)$ are added. After some algebraic manipulations and replacing p_g by $p_w + P_C(S_w)$ in the left side of the combined equation, the following equation in p_w (called pressure equation) is obtained,

$$
\begin{aligned}
& B_g\Big[\nabla \cdot (\underline{\kappa}(\frac{\kappa_{rg}}{B_g\eta_g}(\nabla p_w - \rho_g g\nabla D) + \frac{R_s\kappa_{rw}}{B_w\eta_w}(\nabla p_w - \rho_w g\nabla D) + \frac{\kappa_{rg}}{B_g\eta_g}\nabla P_C))\Big] \\
& + (B_w - R_s B_g)\Big[\nabla \cdot (\underline{\kappa}\frac{\kappa_{rw}}{B_w\eta_w}(\nabla p_w - \rho_w g\nabla D))\Big] \\
& + B_g\frac{q_g}{\rho_g^{SC}} + (B_w - R_s B_g)\frac{q_w}{\rho_w^{SC}} = \phi c_t\frac{\partial p_w}{\partial t},
\end{aligned}
\tag{9}
$$

where c_t is the total compressibility $c_t = c_f + S_g c_g + S_w c_w$ with:

Formation compressibility: $c_f = \dfrac{1}{\phi}\dfrac{d\phi}{dp_w}$,

Gas compressibility: $c_g = -\dfrac{1}{B_g}\dfrac{dB_g}{dp_w}$,

Water compressibility: $c_w = -\dfrac{1}{B_w}\dfrac{dB_w}{dp_w} + \dfrac{B_g}{B_w}\dfrac{dR_s}{dp_w}$,

In the BOAST simulator, the nonlinear differential equations (9) and (7) are discretized applying a backward finite difference scheme in a block centered grid. The discretized equations are linearized evaluating the pressure and saturation dependent coefficients (PVT parameters, viscosities, relative permeabilities and capillary pressure) using the pressure and saturation values of the previous time step. First, the pressure equation (9) is solved implicitly. The Block Successive Over Relaxation method (BSOR) is applied to compute the solution of the resulting linear system. Once the pressures for the new time are obtained, we compute the saturations explicitly from the discretization of equation (7). Consequently, the time step has to be selected according to the stability restrictions (Savioli and Bidner, 2005).

2.2 Fracture Criterion

We apply a criterion based on a *breakdown pressure* (P_{bd}), defined as follows: once pore pressure $p = S_g p_g + S_w p_w$ becomes greater than the breakdown pressure on a certain cell, this cell is fractured, .ie., permeability and porosity are incremented. The *breakdown pressure* can

be computed from the horizontal stress σ_H and the tensile stress of the rock T_0 (Economides and Hill, 1994) as follows,

$$P_{bd} = 3\sigma_{Hmin} - \sigma_{Hmax} + T_0 - p_H, \tag{10}$$

where

$$\sigma_{Hmax} = \sigma_{Hmin} + \sigma_{Tect} \tag{11}$$

being σ_{Tect} the tectonic stress contribution and σ_{Hmin} the minimum horizontal stress obtained from the vertical stress (σ_v) as

$$\sigma_{Hmin} = \frac{\nu}{1-\nu}\sigma_v \tag{12}$$

where ν is the Poisson ratio and σ_v is calculated from formation density (ρ_f) as

$$\sigma_v = g \int_0^H \rho_f \, dz. \tag{13}$$

with H indicating the formation depth and g the gravity constant.

3 NUMERICAL RESULTS

The objective of this work is to analize the capacity of a black oil model coupled with a simple fracture criterion to simulate fracture propagation during water injection.

In the numerical experiments, we consider a portion of a tight gas reservoir of 16.5 m × 30 m × 16.5 m. It is discretized using a 150 × 180 × 150 mesh. The mesh is uniform, but it is refined around the injection point, i.e., there is a 120 × 120 × 120 zone where $\Delta x = \Delta y = \Delta z = 0.2 ft = 0.061 \, m$, outside this zone $\Delta x = \Delta y = \Delta z = 1 ft = 0.3048 \, m$.

The reservoir has natural fractures that are located in a 2D plane (y-z) near the injection point. Figure 1 illustrates this description.

Figure 1: Porosity distribution in a 2D section of the reservoir

The figure shows the porosity map in a portion of that 2D plane, corresponding to the refined grid mentioned above. We can observe two natural fractures and the injection point in yellow.

Matrix permeability and porosity are considered constant, $\kappa_m = 0.0001$ mD and $\phi_m = 0.1$, respectively. In natural fractures permeability and porosity are $\kappa_f = 10$ mD and $\phi_f = 0.4$. Finally, when the cell is hydraulically fractured, the properties become $\kappa_F = 10000$ mD and $\phi_F = 0.9$. Due to the low matrix permeability value, we need a small time increment to achieve convergence, $\Delta t = 0.5\,s$. Properties are updated every $10\,s$.

Besides, we assume a fractal distribution of the breakdown pressure P_{bd} based on the von-Kármán correlation function (Frankel and Clayton, 1986), as shown in Figure 2.

Figure 2: Breakdown pressure distribution in a 2D section of the reservoir

The initial water saturation is $S_w = 0.1$. Water is injected at a constant flow rate of 0.14 m³/s.

The time evolution of the fracking process can be seen in Figures 3-11. Figures 3-5 show the reservoir pressure map for times 10 seg, 50 seg and 160 seconds after injection, respectively, while the corresponding water saturation evolution is shown in Figures 6-8. Besides in Figures 9-11 permeability values are plotted, as a way to represent the fracking procedure. Comparing Figures 9-11 with Figures 3-5, we can see that permeability maps follow pressure distribution as a consequence of the fracking criterion. Water front advance is a bit delayed as Figures 6-8 illustrate. The location of this front is very important to predict how far the sand or ceramic materia arrives in order to maintain the fracture open.

In all these figures we can observe the influence of natural fractures during the injection process. Pressure increases around the injection point and, consequently, permeability changes in those cells. But once a natural fracture is reached, the hydraulic fracture follows its behavior: the influence of the lower natural fracture is illustrated in Figures 9-10 (corresponding to pressure maps Figures 3-4) while Figure 11 (corresponding to pressure map Figure 5) shows the influence of the higher natural fracture.
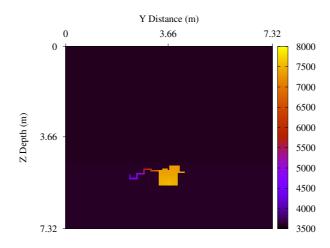
Figure 3: Pressure distribution in the 2D section after 10 seconds of injection
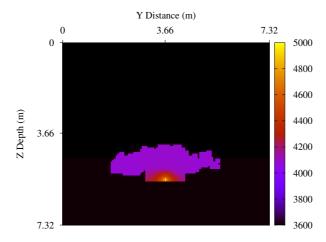

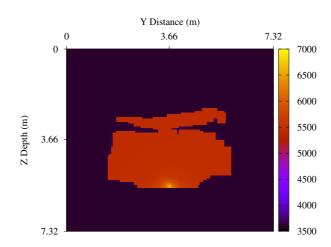Figure 4: Pressure distribution in the 2D section after 50 seconds of injection

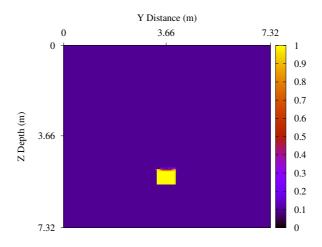Figure 5: Pressure distribution in the 2D section after 160 seconds of injection

Figure 6: Saturation distribution in the 2D section after 10 seconds of injection
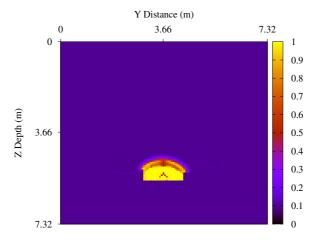

Figure 7: Saturation distribution in the 2D section after 50 seconds of injection
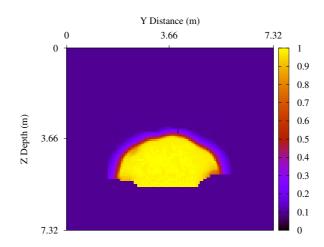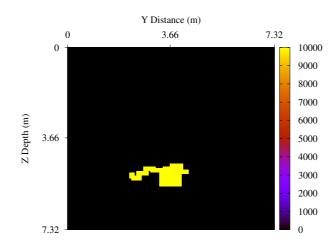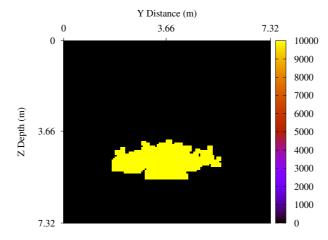

Figure 8: Saturation distribution in the 2D section after 160 seconds of injection

Figure 9: Permeability distribution in the 2D section after 10 seconds of injection

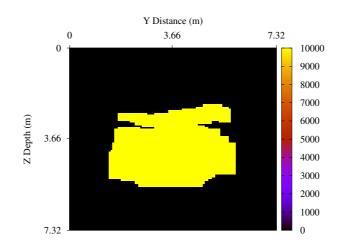Figure 10: Permeability distribution in the 2D section after 50 seconds of injection

Figure 11: Permeability distribution in the 2D section after 160 seconds of injection

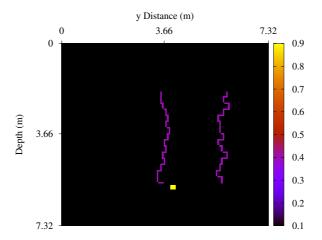In the second example we consider that the natural fractures are located vertically, as Figure 12 shows.

Figure 12: Porosity distribution in a 2D section of the reservoir

Figures 13-14 show the reservoir pressure distribution for times 20 seconds and 160 seconds after injection, while the corresponding water saturation and permeability evolutions are shown in Figures 15-16 and Figures 17-18, respectively.

A behavior analogous to that of the first example is obtained. Figures 13 and 17 illustrate the influence of the left natural fracture, while in Figures 14 and 18 the right fracture also affects the evolution of the fracking process. Note that the left natural fracture affects earlier this behavior because it is closer to the injection point, as Figure 12 shows. Again, water front advance is delayed. This behavior is in agreement with planar fracture geometry induced from actual microseismic data.

4 CONCLUSIONS

This work presents a simple model of generation of hydraulic fractures in unconventional reservoirs. This model uses a public domain numerical simulator, the BOAST multiphase fluid flow simulator, combined with a simple fracture criterion, based on a $breakdown\,pressure$ (P_{bd}). The numerical results show that this approach is able to reproduce the propagation of fractures in a two-phase reservoir with low porosity and permeability, giving the distribution of pressures, saturations and permeabilities during the fracking process. Besides it allows to analyze the influence of natural fractures, and in the same way, it can be applied to study the influence of other different factors that could take part in the fracking process to enhance gas or oil production. This work is a starting point that will allow us to continue working not only in the prediction of the propagation of hydraulic fractures in different porous media, but also in the generation of seismic images produced by the fracture events simulated by this model.
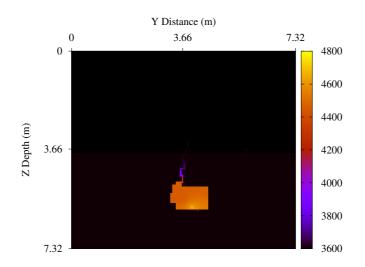
5 ACKNOWLEDGMENTS

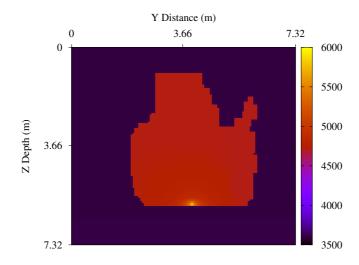Figure 13: Pressure distribution in the 2D section after 20 seconds of injection

Figure 14: Pressure distribution in the 2D section after 160 seconds of injection

REFERENCES

Aziz K. and Settari A. *Petroleum Reservoir Simulation*. Elsevier Applied Science Publishers, Great Britain, 1985.

Bear J. *Dynamics of Fluids in Porous Media*. American Elsevier Publishing Company, New York, USA, 1972.

Bidner M.S. *Propiedades de la roca y los fluidos en reservorios de petroleo*. EUDEBA, Buenos Aires, Argentina, 2001.

Economides M.J. and Hill A.D. *Petroleum Production Systems*. Prentice Hall PTR, New Jersey, USA, 1994.

Fanchi J. *Principles of Applied Reservoir Simulation*. Gulf Professional Publishing Company, Houston, Texas, 1997.

Frankel A. and Clayton R. Finite difference simulation of seismic wave scattering: implications for the propagation of short period seismic waves in the crust and models of crustal heterogeneity. *J. Geophys. Res.*, 91:6465–6489, 1986.
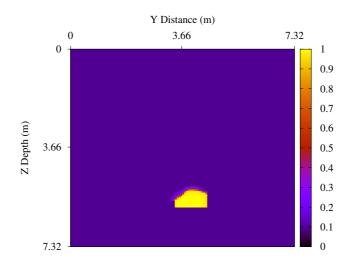
Figure 15: Saturation distribution in the 2D section after 20 seconds of injection

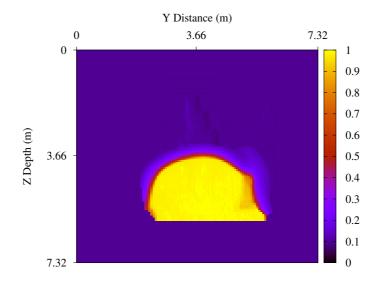Figure 16: Saturation distribution in the 2D section after 160 seconds of injection

Jones K. On the differential form of darcy's law. *J. Geophys. Res.*, 2:731–732, 1962.

Nagel N., Zhang F., Sanchez-Nagel M., and Lee B. Numerical study of interaction between hydraulic fracture and discrete fracture network. In A. Bunger, J. McLennan, and R. Jeffrey, editors, *Quantitative Evaluation of Completion Techniques on Influencing Shale Fracture Complexity*. INTECH, 2013.

Pak A. and Chan D. Numerical modeling of hydraulic fracturing in oil sands. *Scientia Iranica*, 15:516–535, 2008.

Riahi A. and Damjanac B. Numerical study of interaction between hydraulic fracture and discrete fracture network. In A. Bunger, J. McLennan, and R. Jeffrey, editors, *Effective and Sustainable Hydraulic Fracturing*. INTECH, 2013.

Savioli G. and Bidner M.S. Simulation of the oil and gas flow toward a well - a stability analysis. *Journal of Petroleum Science and Engineering*, 48:53–69, 2005.

Sena A., Castillo G., Chesser K., Voisey S., Estrada J., Carcuz J., Carmona E., and Hodgkins
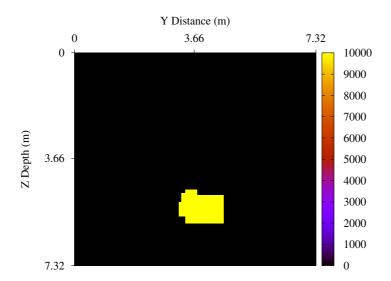
Figure 17: Permeability distribution in the 2D fractured section after 20 seconds of injection
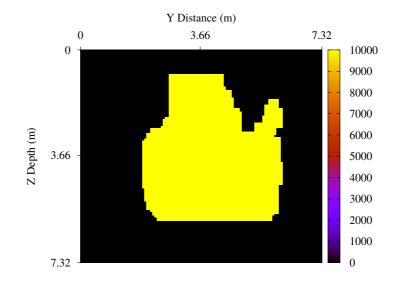

Figure 18: Permeability distribution in the 2D fractured section after 160 seconds of injection

P. Seismic reservoir characterization in resource shale plays: Stress analysis and sweet spot discrimination. *The Leading Edge*, pages 758–764, 2011.

Wang H. and Zhang S. *Numerical computation of hydraulic fracturing design*. Beijing: Petroleum Industry Press, Beijing, China, 1998.

Wangen M. Finite element modeling of hydraulic fracturing on a reservoir scale in 2d. *Journal of Petroleum Science and Engineering*, pages 274–285, 2011.

Zhao J., Li Y., Wang S., Jiang Y., and Zhang L. Simulation of complex fracture networks influenced by natural fractures in shale gas reservoir. *Natural Gas Industry B*, pages 89–95, 2014.